

Anodic Dissolution in Sulfuric Acid Pickling Solutions of the API Pipeline X70 Grade Steel

El-Sayed M. Sherif^{1,2,*} and Asiful H. Seikh¹

¹College of Engineering, King Saud University, P.O. Box - 800, Riyadh 11421, Saudi Arabia

²Electrochemistry and Corrosion Laboratory, Department of Physical Chemistry, National Research Centre (NRC), Dokki, 12622 Cairo, Egypt

*E-mail: esherif@ksu.edu.sa; emsherif@gmail.com

Received: 14 August 2014 / Accepted: 13 October 2014 / Published: 17 November 2014

The anodic dissolution of API X70 pipeline grade steel was investigated after different exposure periods of time and different temperatures in 1.0 M H₂SO₄ pickling solutions using optical microscopy, electrochemical impedance spectroscopy (EIS), and potentiodynamic polarization measurements. The EIS and polarization measurements showed clearly that the increase of immersion time increases the anodic and cathodic currents and corrosion current density decreased both the solution and polarization resistances for the steel in the sulfuric acid solution. It was also found that increasing the solution temperature in the range from 20 °C to 60 °C highly increased the corrosion of the API X70 pipeline steel due to the faster and contentious dissolution of X70 steel with temperature. Results together were in good agreement with each other confirming that X70 steel suffers sever corrosion in H₂SO₄ solution and that effect increases with increasing the exposure period and temperature.

Keywords: Acidic pickling solutions, API steels, Corrosion, EIS, Polarization

1. INTRODUCTION

API pipeline steels are high-strength low alloy (HSLA) steel grades due to its high strength and toughness, good weldability and formability [1-3]. These steels have wide range of applications in chemical processing such as chemical and allied industries for the handling of acid, alkali and salt solutions, construction materials and metal processing equipment, oil / gas storage tanks, marine applications and transportation pipelines [4-6]. Oil and gas transport pipelines are manufactured by welding segments of carbon steel pipe. This process alters the microstructure of the materials causing local variations in the composition and phases. These changes increase the dissimilarity of the base/weld metal combination and can cause galvanic corrosion [7].

Henthorne and Parkins [8] observed that corrosion occurs along grain boundaries in the absence of stress, and that anodic polarization can cause virtual disintegration of unstressed carbon steel by intergranular corrosion. Furthermore, this work [8] indicated that the corrosion is related to the presence of carbon or carbides at the ferrite grain boundaries. The temperature and holding times influence the ferrite carbon solubility and carbon segregation to grain boundaries [9]. The service life of pipeline steels is affected not only by the transferred fluid or gas but also by the environmental conditions under which they operate. Corrosion is a serious problem in steel pipelines and is one of the main reasons in affecting the service life of the pipeline. This is due to its extremely expensive cost and the time lost in repairing or replacing or even maintaining these pipes [10-15]. The corrosion of steel in acidic solutions is an industrial concern that has received a considerable amount of attention [16,17].

Several investigators have reported [18-21] that the pipeline failure usually occurs not only as a result of uniform corrosion but also in the form of localized attack, generally as pitting or galvanic corrosion of welds. These forms of attack can cause pipeline degradation that can lead to spillage of products resulting in environmental catastrophes. The water content associated with the oil production process has been found to be a significant factor in the internal corrosion of steel pipelines because the water contains many corrosive agents such as carbon dioxide, hydrogen sulphides, organic acids and salts [20,21].

In this work, we reported the electrochemical corrosion behaviour of the API 5L X70 pipeline steel in 1.0 M H₂SO₄ pickling solutions after different exposure periods of time, namely 10 min, 60 min, and 24 h. The aim was also extended to investigate the effect of raising the temperature of the pickling solution from 20 °C to 60 °C on the activation of the X70 steel surface. Optical microscopy, electrochemical impedance spectroscopy, and potentiodynamic polarization measurements were employed to achieve this investigation.

2. EXPERIMENTAL DETAILS

2.1. Materials and Chemicals

A hot-rolled plate of 15 mm thickness sheet of API X70 5 L pipeline steel was supplied by the Saudi Arabian Basic Industries Corporation (SABIC). The typical chemical compositions of the elements present in the steel sheet in wt. % are listed in Table 1. For the electrochemical measurements, the X70 rods with dimensions of 1×1×0.5 cm were cut from the delivered steel sheet. A stock solution of 1.0 M sulfuric acid was prepared from the concentrated acid solution (96%) that was purchased from Merck and was used as received.

Table 1. Chemical compositions (in wt. %) for the employed API X70 5L pipeline steel.

Element	C	Si	Mn	P	S	Al	Ti	Cu	Cr	Mo	Nb + V	Ni
Wt. %	0.05	0.25	1.5	0.01	0.002	0.04	0.018	0.05	0.014	0.2	< 0.09	0.02

2.2. Electrochemical cell

A conventional three-electrode cell accommodates for 200 mL solution was employed in this study to perform the electrochemical measurements. The API X70 5L pipeline steel, Ag/AgCl (in saturated KCl), and a platinum foil were used as the working, reference, and counter electrode, respectively. One face of the steel working electrode was drilled and welded with copper wire and was then embedded into two-component epoxy resin and mounted in a glass holder. Where, the other face was left to be polished and exposed to the acid solution. Prior to each experimental measurement, the exposed surface of the steel electrode (of area 100 mm²) was wet ground with silicon carbide abrasive papers up to 1000 grit, rinsed with ethanol and air dried.

2.3. Optical microscopy investigations

One of the surfaces of the API X70 5L pipeline steel was mechanically ground on the silicon carbide abrasive papers sequentially on 60, 120, 240, 320, 400, 600, and 1000 grit silicon carbide papers and polished on a Sylvet cloth using coarse and fine Geosyn- Grade I slurry of Al₂O₃. This surface was cleaned, washed by water, alcohol, dried in air and then etched in 2% Nital solution (2% HNO₃ in ethyl alcohol). The etched specimen was observed by XJL-03 model metallographic microscope and the microstructure was taken with the help of a Camera fitted with the microscope.

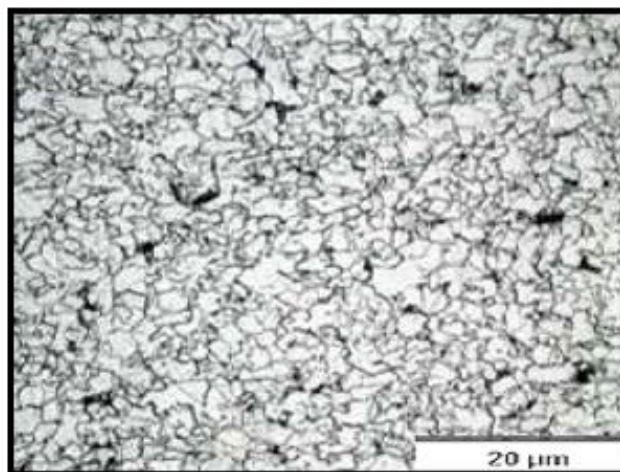


Figure 1. Optical micrograph of the API X70 5L pipeline steel employed in this investigation.

2.4. Electrochemical measurement techniques

Electrochemical experiments were performed using an Autolab Potentiostat (PGSTAT20, computer controlled) operated by the general purpose electrochemical software (GPES) version 4.9. The electrochemical impedance spectroscopy (EIS) tests were performed at corrosion potentials over a frequency range of 100 kHz to 100 mHz, with an ac wave of ± 5 mV peak-to-peak overlaid on a dc bias

potential, and the impedance data were collected using Powersine software at a rate of 10 points per decade change in frequency. The best equivalent circuit of Nyquist plots was obtained by fit and simulation method. The potentiodynamic polarization curves were obtained by scanning the potential in the forward direction against the Ag/AgCl reference electrode and at a scan rate of 0.001 V/s. All measurements were recorded at the free corrosion potential that was obtained after immersing the working electrode for 10 min, 60 min, and 24 h in the sulfuric acid test solutions. All electrochemical experiments were recorded in fresh solution and new steel surface and were repeated for three times to ensure the reliability and reproducibility of the obtained data.

3. RESULTS AND DISCUSSION

3.1. Optical microscopy and microstructure investigations

The microstructure of API steel X70 was investigated using the optical microscopy image shown in Fig. 1. It is clearly seen from the micrograph that the microstructure of the X70 steel is composed of acicular ferrite (AF) with polygonal ferrite (PF) and quasi polygonal ferrite (QPF) matrix (α). Moreover, there are some grain boundary carbides in which the acicular ferrite is the dominant phase.

3.2. Electrochemical impedance spectroscopy (EIS) measurements

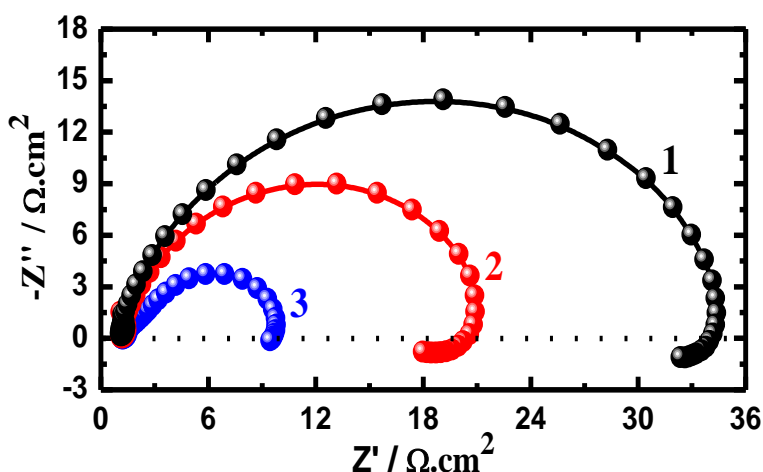


Figure 2. Typical Nyquist plots obtained for X70 5L pipeline steel samples after (1) 10 min, (2) 60 min and (3) 24 h immersion in 1.0 M H_2SO_4 solutions at room temperature.

In order to report the kinetic parameters for electron transfer reactions at the interface of the X70 pipeline steel and the sulfuric acid corrosive test solution, the EIS measurements were carried out after varied exposure periods of time and different temperatures. Where, the EIS technique has been successfully used to explain the mechanism of corrosion and corrosion control for metals and alloys in different aggressive environments [22-24]. Fig. 2 shows the typical Nyquist plots obtained for the API

X70 steel after its immersion at room temperature in 1.0 M H_2SO_4 solution for (1) 10 min, (2) 60 min and (3) 24 h, respectively. The Nyquist plots depicted in Fig. 2 showed only one depressed semicircle whose diameter decreased with increasing the time from 10 min to 60 min and further to 24 h. This decrease in the diameter of the semicircle with increasing the immersion time was resulted due to the increase of the corrosiveness attack of the sulfuric acid solution towards the steel surface, which in turn increased its dissolution. It has been reported [25,26] that the deviation of the semicircle from the ideal shape is due to the dispersion of the frequency and the heterogeneities of the surface as well as the resistant to mass transport. The capacitance loop intersects the real axis at higher and lower frequencies. Where, at high frequency end the intercept corresponds to the solution resistance (R_s) and at lower frequency end corresponds to the sum of R_s and the polarization resistance (R_p).

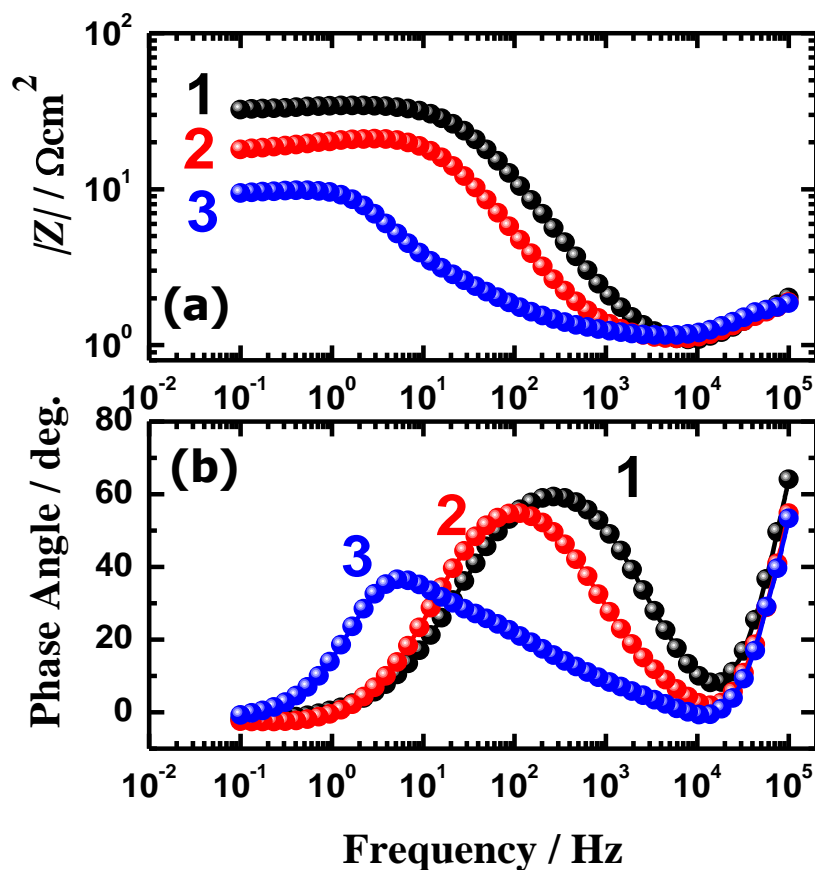


Figure 3. (a) Bode impedance and (b) Bode phase angle plots obtained for the API X70 5L pipeline steel after (1) 10 min, (2) 60 min and (3) 24 h immersion in 1.0 M H_2SO_4 solutions at room temperature.

In order to confirm the behavior of the obtained Nyquist data for the steel after its immersion for the reported immersion times, the variation of the Bode impedance as well as the Bode phase angle with changing of the applied frequency were also plotted. Fig. 3 shows (a) Bode impedance ($|Z|$) and (b) Bode phase angle (ϕ) plots obtained for the API X70 5L pipeline steel after its immersion in 1.0 M H_2SO_4 solutions for (1) 10 min, (2) 60 min, and (3) 24 h, respectively. It is clearly seen from Fig. 3(a) that the impedance of the interface for the steel increased with increasing frequency, while

significantly decreased with increasing the immersion time. It has been reported [27-29] that the high impedance at lower frequency values indicates on the passivation of the surface; this means that the decrease of the impedance of the interface with increasing the immersion time was due to the decreased corrosion resistance and in turn the increased dissolution of the steel with time in the acid solution.

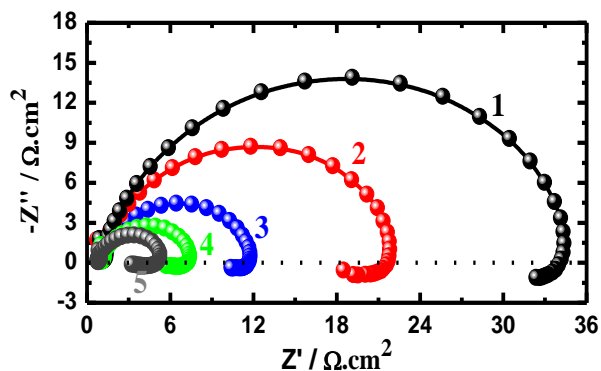


Figure 4. Nyquist plots obtained for the API X70 steel in 1.0 M H₂SO₄ solutions at (1) 20 °C, (2) 30 °C, (3) 40 °C, (4) 50 °C and (5) 60 °C, respectively.

As well as, Fig. 3(b) indicates that the increase of immersion time decreased the maximum degree of the phase angle, which confirms the data recorded in Fig. 2 and Fig. 3(a) that the increase of immersion time increases the dissolution of the X70 steel in the sulfuric acid pickling solutions under investigations.

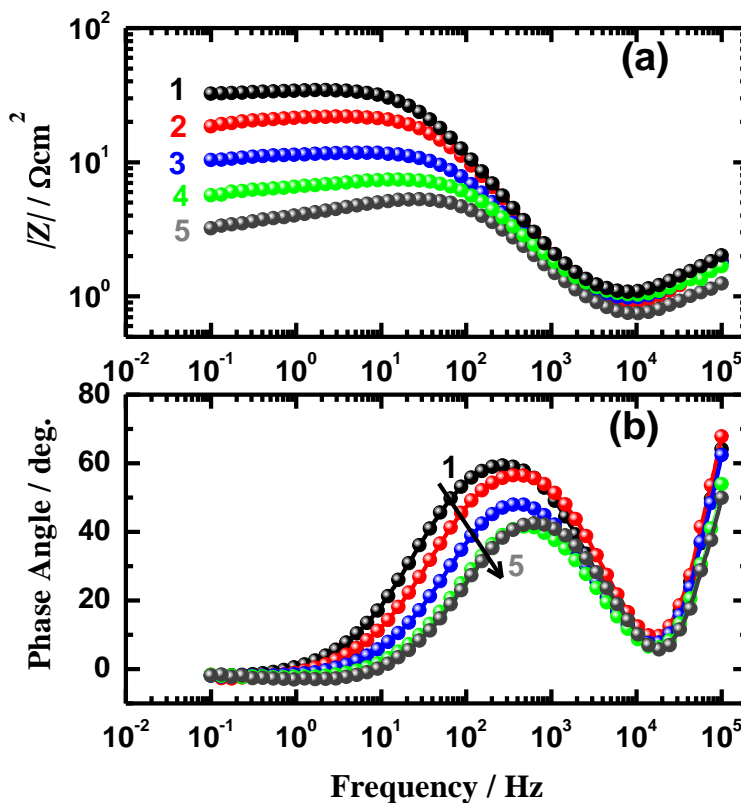


Figure 5. (a) Bode impedance and (b) Bode phase angle plots obtained for the API X70 steel in 1.0 M H₂SO₄ solutions at (1) 20 °C, (2) 30 °C, (3) 40 °C, (4) 50 °C and (5) 60 °C, respectively.

The EIS technique was also used to report the effect of increasing the temperature of the sulfuric acid solution on the electrochemical corrosion behavior of the API X70 pipeline steel. Typical Nyquist plots obtained for X70 steel in 1.0 M H₂SO₄ solutions at (1) 20 °C, (2) 30 °C, (3) 40 °C, (4) 50 °C and (5) 60 °C, respectively are shown in Fig. 4. These Nyquist spectra were followed by drawing the change of the Bode impedance of the interface and the Bode phase angle at the same solutions temperature and the data are depicted in Fig. 5(a) and Fig. 5(b), respectively. It is obviously seen from the EIS results that increasing the solution temperature from 20 °C to 60 °C decreased the diameter of the obtained semicircle, Fig. 4. This effect also decreased the values of $|Z|$, as well as the maximum degree of ϕ . This indicates that the increase of temperature decreases the corrosion resistance of the X70 steel and thus increases its dissolution in the acid test solution, where the increase of temperature increases the reactivity of the steel surface and thus accelerates its corrosion as has been reported previously for similar studies on pipeline steels [12,15,17,30].

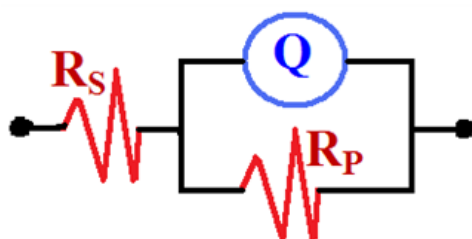


Figure 6. The equivalent circuit model used to fit the experimental data shown in Fig. 2 and Fig. 4.

Table 2. EIS parameters of the API pipeline X70 steel after its immersion in 1.0 M H₂SO₄ for 10 min, 60 min, and 24 h, respectively at room temperature.

time	EIS parameters			
	$R_s / \Omega \text{ cm}^2$	CPE / μMho	N	$R_p / \Omega \text{ cm}^2$
10 min	1.3	281	0.92	34.0
60 min	1.2	542	0.88	20.5
24 h	1.1	8940	0.83	9.60

The data presented in the Nyquist plots shown in Fig. 2 for the X70 steel after different immersion periods of time as well as those shown in Fig. 4 after different solution temperatures were best fitted to the equivalent circuit shown in Fig. 6 and the values of the parameters of this circuit are listed in Table 2 and Table 3, respectively. According to the usual convention, the EIS parameters of the equivalent circuit can be defined as follows; R_s represents the solution resistance, R_p is the polarization resistance and can also be defined as the charge transfer resistance, and Q is the constant phase elements (CPEs). It is clearly seen from Table 2 that the values recorded for R_s and R_p decreased with increasing the immersion time. This confirms that the X70 suffers more corrosion due

to the decreased corrosion resistance and confirm also the decrease of the diameter of the semicircle shown in Fig. 2 with increasing the time of exposure. Furthermore, decreasing the values of R_s and R_p that are listed in Table 3 indicates that the surface of X70 steel gets activated with increasing temperature, which reflects on the increase of its dissolution and the decrease of its corrosion resistance. On the other hand, the values of Q were found to increase both with increasing the immersion time (Table 2) and the temperature of the sulfuric acid solution (Table 3). Here, Q with their n values almost between 0.92 and 0.81, i.e. close to unity, represent impure double layer capacitor; the increase of its values was expected to cover up the charged surfaces of the steel as a result of the irregularities of these surfaces due to its increased dissolution in 1.0 M H_2SO_4 solutions [31]. The EIS measurements collectively reveal that the increase of immersion time as well as temperature remarkably increase the corrosion of the investigated X70 steel grade in the sulfuric acid solution.

Table 3. EIS parameters obtained for the API X70 pipeline steel in 1.0 M H_2SO_4 solutions at different temperatures.

Temp.	EIS parameters			
	$R_s / \Omega \text{ cm}^2$	CPE / μMho	n	$R_p / \Omega \text{ cm}^2$
20 °C	1.30	281	0.92	34.00
30 °C	1.08	298	0.89	21.80
40 °C	0.93	335	0.86	11.20
50 °C	0.85	359	0.84	6.70
60 °C	0.74	398	0.81	4.80

3.3. Potentiodynamic polarization measurements

Polarization is a powerful technique that has been employed to understand the corrosion and corrosion protection of metals and alloys in harsh environments. We have been successfully using the polarization method in investigating the corrosion and corrosion inhibition of different metals and alloys in varied corrosive media [32-34]. Fig. 7 shows the potentiodynamic polarization curves obtained for the API X70 pipeline steel after its immersion for (1) 10 min, (2) 60 min and (3) 24 h, respectively in 1.0 M H_2SO_4 solution at room temperature. The values of the corrosion current densities (j_{CORR}), corrosion potential (E_{CORR}), cathodic (β_c) and anodic (β_a) Tafel slopes, and polarization resistance (R_p) obtained from the curves shown in Fig. 7 are listed in Table 4. The values of the Tafel slopes, β_c and β_a , were determined according to our previous study [34]. The values of j_{CORR} and E_{CORR} were obtained from the extrapolation of anodic and cathodic Tafel lines located next to the linearized current regions [32-34]. The R_p values were calculated as reported in our previous investigations [1,32-34];

Fig. 7 shows that the increase of potential in the anodic side regularly increased the anodic current due to the dissolution of iron (Fe^0), which is the base metal in the API X70 steel to iron cations (Fe^{2+}) as follows;



The ferrous cations, Fe^{2+} , further oxidized under the increase of potential and the aggressiveness action of the sulfuric acid solution in ferric cations, Fe^{3+} , according the following reaction;



The electrons produced from the previous reactions were consumed at the cathode as a result of the hydrogen evolution reaction as follows;

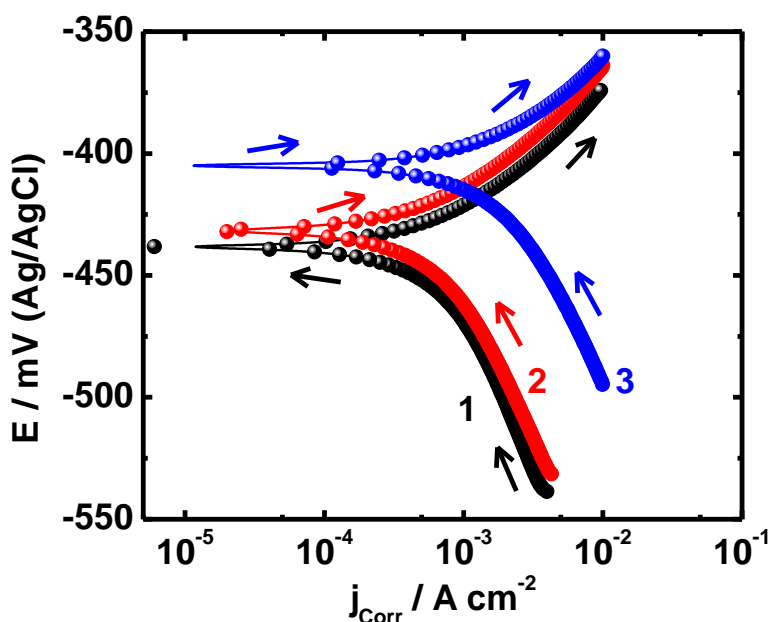


Figure 7. Potentiodynamic polarization curves obtained for X70 5L pipeline steel samples after (1) 10 min, (2) 60 min and (3) 24 h immersion in 1.0 M H_2SO_4 solutions at room temperature.

Table 4. Potentiodynamic polarization parameters obtained for the API X70 steel after 10 min, 60 min and 24 h immersion in 1.0 M H_2SO_4 at room temperature.

time	Polarization parameters				
	$\beta_c / mVdec^{-1}$	$\beta_a / mV/dec^{-1}$	E_{Corr} / mV	$j_{Corr} / \mu A cm^{-2}$	$R_p \Omega cm^2$
10 min	20.24	27.65	-438	157.8	32.15
60 min	30.15	42.28	-425	288.3	26.51
24 h	22.23	25.73	-405	421.3	12.29

It is also seen from Fig. 7 that the lowest anodic and cathodic currents were recorded for the steel after its immersion for 10 min in the acid solutions at room temperature. Increase the time of immersion to 60 min and further to 24 h led to increasing the cathodic and anodic currents as a result of the increased corrosiveness action of the acid with time. Table 4 also depicts that the increase of immersion time increased the values of j_{Corr} and R_{Corr} as well as decreased the values of R_p , which confirms that the dissolution of X70 increases with increasing the exposure time. The values of E_{Corr} were also shifted to the less negative direction with the increase of immersion time before measurements. The positive shift in the values of E_{Corr} indicates that the anodic process is much more affected than the cathodic one [35]. It was also reported [36] that the increased dissolution of the steel was due to the ability of the sulfuric acid molecules in preventing the steel surface to form layers of oxide and/or corrosion products that in turn allows the surface to suffer a continuous corrosion.

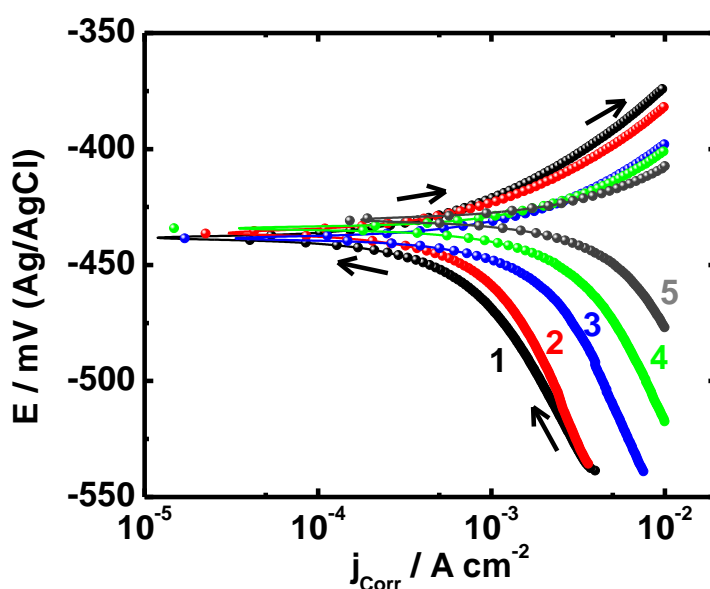


Figure 8. Potentiodynamic polarization curves obtained for the API X70 5L pipeline steel in 1.0 M H_2SO_4 solutions (1) 20 °C, (2) 30 °C, (3) 40 °C, (4) 50 °C and (5) 60 °C, respectively.

Table 5. Corrosion parameters obtained for the potentiodynamic polarization for the API X70 pipeline steel in 1.0 M H_2SO_4 at different temperature.

Polarization parameters					
Temp	$\beta_c / \text{mVdec}^{-1}$	$\beta_a / \text{mVdec}^{-1}$	$E_{\text{Corr}} / \text{mV}$	$j_{\text{Corr}} / \mu\text{A cm}^{-2}$	$R_p \Omega \text{cm}^2$
20 °C	20.24	27.65	-443	157.8	32.15
30 °C	23.54	40.42	-439	294.5	21.94
40 °C	22.97	29.37	-436	498.9	11.22
50 °C	20.76	29.27	-434	711.2	7.42
60 °C	15.39	22.84	-430	967.9	4.12

In order to shed more light on the effect of increasing the temperature of the 1.0 M H₂SO₄ solution on the corrosion of X70, the polarization measurements were also carried out. Fig. 8 shows the potentiodynamic polarization curves obtained for the API X70 5L pipeline steel in 1.0 M H₂SO₄ solutions (1) 20 °C, (2) 30 °C, (3) 40 °C, (4) 50 °C and (5) 60 °C, respectively. The corrosion parameters obtained from Fig. 8 are listed in Table 5. It is obvious from Fig. 8 and Table 5 that the increase of temperature significantly increased the anodic and cathodic currents and the values of j_{Corr} and R_{Corr} . This effect was found to also decreased the values of R_p and slightly shifted the values of E_{Corr} toward the less negative direction. The increase of the anodic and cathodic currents and the values of j_{Corr} and R_{Corr} and conjunctly the decrease of R_p indicate that the steel suffers more corrosion with increasing temperature. Furthermore, the little change of β_a and β_c values listed in Table 5 with increasing temperature of the acid solution proves that there was a little change in the mechanism of corrosion of X70 with increasing temperature.

3.4. Effect of temperature on the activation energy of steel

In addition to the data obtained from the EIS and polarization measurements, we also calculated the activation energy (E_a) for the API X70 pipeline steel in the acid solution (1.0 M H₂SO₄) at the different temperature from the Arrhenius equation as follows [37],

$$\ln(j_{\text{Corr}}) = B - \left(\frac{E_a}{RT} \right) \tag{4}$$

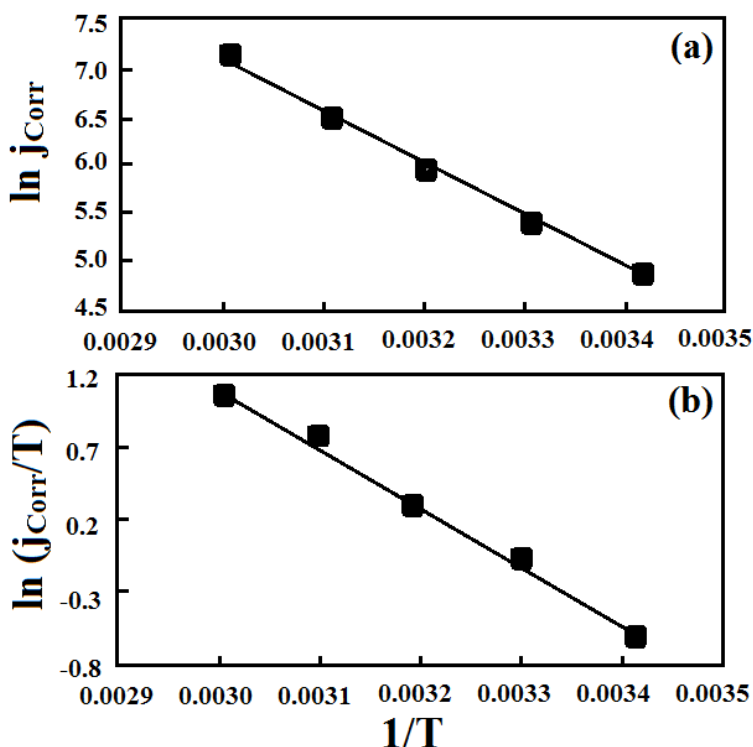


Figure 9. (a) Arrhenius and (b) $\ln(j_{\text{Corr}}/T)$ vs. $1/T$ plots for the dissolution of the API X70 5L pipeline steel after its immersion for 30 min in 1.0 M sulphuric acid solutions after different temperatures.

Here, B is a constant that depends on the metal type and R is the universal gas constant. The plot of $\ln(j_{\text{Corr}})$ versus the reciprocal of absolute temperature ($1/T$) gives a straight line whose slope = $-(E_a / R)$, from which the activation energy values for the corrosion process were calculated. The Arrhenius plot for the API 5L X70 pipeline steel rode is shown in Fig. 9a. The values for the enthalpy (ΔH) of activation and the entropy (ΔS) of activation were calculated from transition state theory according to the following equation [37];

$$j_{\text{Corr}} = \left(\frac{RT}{Nh} \right) \exp \frac{\Delta S}{R} \exp \frac{-\Delta H}{RT} \quad (5)$$

According to universal definition, h is the Planck's constant and N is the Avogadro's number.

The relation between $\ln(j_{\text{Corr}}/T)$ and $1/T$ for the API 5L X70 pipeline steel electrode was also plotted as depicted in Fig. 9b. It is clearly seen from Fig. 9b that the plotted data show a straight line; the slope value of this line represents $-\Delta H/R$. Moreover, the intercept represents a value equal to $\ln(R/Nh) + \Delta S/R$. The values of E_a , ΔH , and ΔS were calculated to be 36.76, 34.16, and -85.38 KJ/mol, respectively. The value of 36.76 kJ/mol obtained for the X70 steel as activation energy, E_a confirms that the whole corrosion process is controlled by surface reaction [38]. Furthermore, the negative value recorded ΔS , -85.38 reveal also that the activated complex in the rate-determining step represents is under an associative mechanism and there is a decrease in randomness takes place on going from reactants to the activated complex [39]. This confirms that the increase of the sulfuric acid temperature from 20 °C to 60 °C increases the activation parameters of X70 pipeline steel, which lead to increasing its surface reactivity and in turn increases its dissolution. These results of activation energy are thus in good agreement with the data obtained from EIS and polarization measurements; all confirm that the increase of temperature increases the corrosion of the steel in 1.0 M H_2SO_4 solutions.

4. CONCLUSIONS

The electrochemical corrosion behavior of the API X70 5L pipeline steel grade after its immersion for 10 min to 60 min and further to 24 h in 1.0 M sulfuric acid (H_2SO_4) pickling solutions was investigated. The effect of increasing the temperature of the acid solution from 20 °C to 60 °C on the anodic dissolution of the X70 steel was also reported. The work was performed using different experimental techniques such as optical microscopy, electrochemical impedance spectroscopy (EIS), and potentiodynamic polarization measurements. The study was also complemented by calculating the activation (E_a), enthalpy (ΔH) and entropy (ΔS) of activation resulted from the corrosion of X70 versus the reciprocal of the absolute temperature. It has been found that the increase of time of immersion decreases the resistance of the steel surface against corrosion and indicated by EIS plots. The polarization data confirmed also that the corrosion of X70 in 1.0 M H_2SO_4 solutions increases with time due to increasing the anodic and cathodic currents and corrosion current density (j_{Corr}). Where, this effect also decreased the values of polarization resistance (R_p). The increase of the acid temperature from 20 °C to 60 °C was found to significantly increasing the corrosion of the X70 steel as a result of the accelerated and contentious dissolution of the surface with temperature as indicated from the calculated values of E_a , ΔH , and ΔS . All measurements were in good agreement confirming that

the X70 steel corrodes faster in 1.0 M H₂SO₄ solutions with increasing the immersion time to 24 h and raising the temperature of the acid to 60 °C.

ACKNOWLEDGEMENTS

The authors would like to extend their sincere appreciation to the Deanship of Scientific Research at King Saud University for its funding of this research through the Research Group Project No. RGP-160.

References

1. B.Y. Fang, A. Atrens, J.Q. Wang, E.H. Han, Z.Y. Zhu and W. Ke, *J. Mater. Sci.*, 38 (2003) 127.
2. E.-S. M. Sherif and Abdulhakim A. Almajid, *J. Chem.*, 2014 (2014) 1.
3. T. Poornima, J. Nayak, A.N. Shetty, *Port. Electrochim. Acta*, 28 (2010) 173.
4. A. Guenbour, M.A. Hajji, E.M. Jallouli and A. Ben Bachir, *Appl. Surf. Sci.*, 253 (2006) 2362.
5. B. Gu, W. Z. Yu, J.L. Luo, and X. Mao, *Corrosion*, 55 (1999) 312.
6. E.-S.M. Sherif, A.A. Almajid, A.K. Khalil, H. Junaedi and F.H. Latief, *Int. J. Electrochem. Sci.*, 8 (2013) 9360.
7. T. Hemmingsten, H. Hovdan, P. Sanni, and N.O.Aagotnes, *Electrochim. Acta*, 47(2002) 3949.
8. M. Henthorne and R.N. Parkins, *Brit. Corros. J.* 7 (1967) 186.
9. J.Y. Lee and S. M. Lee, *Surf. Coat. Technol.*, 28 (1986) 301.
10. N. Muthukumar, S. Maruthamuthu and N. Palaniswamy, *Colloids Surf. B: Biointerf.*, 53 (2006) 260.
11. B. Gu, J. Luo, and X. Mao, *Corrosion*, 55 (1999) 96.
12. M. A. Migahed, *Prog. Org. Coat.*, 54 (2005) 91.
13. J. W. Graves and E. H. Sullivan, *Mater. Prot.*, 5 (1996) 33.
14. M.C. Zhao, K. Yang and Y.Y. Shan, *Mater. Lett.*, 57 (2003) 1496.
15. S. Nešić, *Corros. Sci.*, 49 (2007) 4308.
16. S. Ghareba and S. Omanovic, *Corros. Sci.*, 52 (2010) 2104.
17. M.A. Hegazy, H.M. Ahmed and A.S. El-Tabei, *Corros. Sci.*, 53 (2011) 671.
18. C.T. Kwok, S.L. Fong, F.T. Cheng and H.C. Man, *J. Mater. Proc. Technol.*, 176 (2006) 168.
19. F.Y. M and W.H. Wang, *Mater. Sci. Eng. A*, 430 (2006) 1.
20. D. Hardie, E. A. Charles and A. H. Lopez, *Corros. Sci.*, 48 (2006) 4378.
21. X. Jiang, Y.G. Zheng and W. Ke, *Corros. Sci.*, 47 (2005) 2636.
22. E.-S. M. Sherif, *J. Mater. Eng. Performance*, 19 (2010) 873.
23. E.-S. M. Sherif, *Int. J. Electrochem. Sci.*, 6 (2011) 2284.
24. E.-S. M. Sherif, *Mater. Chem. Phys.*, 129 (2011) 961.
25. P. Bommersbach, C. Alemany-Dumont, J.P. Millet and B. Normand, *Electrochim. Acta*, 51 (2005) 1076.
26. H.H. Hassan, E. Abdelghani and M.A. Amin, *Electrochim. Acta*, 52 (2007) 6359.
27. F. Mansfeld, S. Lin, S. Kim and H. Shih, *Corros. Sci.*, 27 (1987) 997.
28. D. Gopi, E.-S. M. Sherif, V. Manivannan, D. Rajeswari, M. Surendiran and L. Kavitha, *Ind. Eng. Chem. Res.*, 53 (2014) 4286.
29. Z. Zhang, Shenhao Chen, Yanhui Li, Shuhuan Li and Liang Wanga, *Corros. Sci.*, 51 (2009) 291.
30. A. Hernández-Espejel and M.A. Domínguez-Crespo, *Corros. Sci.*, 53 (2010) 2258.
31. W.B. Johnson and J.R. Macdonald, "Theory in impedance Spectroscopy, experiments and applications," John Wiley & Sons, New York, 2005.
32. E.-S.M. Sherif, *Appl. Surf. Sci.*, 292 (2014) 190.
33. E.-S.M. Sherif, *Ind. Eng. Chem. Res.*, 52 (2013) 14507.

34. E.-S. M. Sherif, H.R. Ammar and A.K. Khalil, *Appl. Surf. Sci.*, 301 (2014) 142.
35. A. El- Sayed, *J. Appl. Electrochem.*, 27 (1997) 193.
36. El-Sayed M. Sherif and A.H. Ahmed, *Synthesis and Reactivity in Inorganic, Metal-Organic, and Nano-Metal Chemistry*, 40 (2010) 365.
37. F. Bentiss, M. Lebrini and M. Lagrenée, *Corros. Sci.*, 47 (2005) 2915.
38. K.K. El-Neami, A.K. Mohamed, I.M. Kenawy and A.S. Fouda, *Monatshefte für Chemie / Chemical Monthly*, 126 (1995) 369.
39. S.S. Abd El-Rehim, M.A.M. Ibrahim and K.F. Khaled, *J. Appl. Electrochem.*, 29 (1999) 593.

© 2015 The Authors. Published by ESG (www.electrochemsci.org). This article is an open access article distributed under the terms and conditions of the Creative Commons Attribution license (<http://creativecommons.org/licenses/by/4.0/>).